HYDROLOGICAL PROCESSES
Hydrol. Process. **29**, 1340–1352 (2015)
Published online 8 July 2014 in Wiley Online Library
(wileyonlinelibrary.com) DOI: 10.1002/hyp.10268

Simulation of stream flow components in a mountainous catchment in northern Thailand with SWAT, using the ANSELM calibration approach

M. A. Bannwarth,[1]* C. Hugenschmidt,[1] W. Sangchan,[1] M. Lamers,[1] J. Ingwersen,[1] A. D. Ziegler[2] and T. Streck[1]

[1] *Institute of Soil Science and Land Evaluation, Biogeophysics Section, University of Hohenheim, Stuttgart, Germany*
[2] *Department of Geography, National University of Singapore, Singapore, Singapore*

Abstract:

Highland agriculture is intensifying rapidly in South-East Asia, leading to alarmingly high applications of agrochemicals. Understanding the fate of these contaminants requires carefully planned monitoring programmes and, in most cases, accurate simulation of hydrological pathways into and through water bodies. We simulate run-off in a steep mountainous catchment in tropical South-East Asia. To overcome calibration difficulties related to the mountainous topography, we introduce a new calibration method, named A Nash–Sutcliffe Efficiency Likelihood Match (ANSELM), that allows the assignment of optimal parameters to different hydrological response units in simulations of stream discharge with the Soil and Water Assessment Tool (SWAT) hydrological model. ANSELM performed better than the Parasol calibration tool built into SWAT in terms of model efficiency and computation time. In our simulation, the most sensitive model parameters were those related to base flow generation, surface run-off generation, flow routing and soil moisture change. The coupling of SWAT with ANSELM yielded reasonable simulations of both wet-season and dry-season storm hydrographs. Nash–Sutcliffe model efficiencies for daily stream flow during two validation years were 0.77 and 0.87. These values are in the upper range or even higher than those reported for other SWAT model applications in temperate or tropical regions. The different flow components were realistically simulated by SWAT, and showed a similar behaviour in all the study years, despite inter-annual climatic differences. The realistic partitioning of total stream flow into its contributing components will be an important factor for using this hydrological model to simulate solute transport in the future.

KEY WORDS hydrologic response simulation; tropical monsoon catchment; Mae Sa; model calibration; ANSELM

Received 20 June 2013; Accepted 4 June 2014

INTRODUCTION

Sustainable use of natural resources is of increasing importance in mountainous regions of South-East Asia where highland agriculture is intensifying rapidly (Schreinemachers and Sirijinda, 2008). Over the last few decades, cropping periods have expanded, and increasing fertilizer and pesticide inputs are required to sustain crop yields and overcome diminishing soil fertility (Bruun *et al.*, 2009). Agrochemical contaminants are of great environmental concern because of their potential to leach into aquatic systems where they may threaten aquatic life and human health (Ziegler *et al.*, 2009; Sangchan *et al.*, submitted). Understanding the threat of these contaminants requires not only carefully planned monitoring programmes but also, in some cases, accurate simulation of contaminant transport into and through stream systems.

Reliable simulations are only possible if the hydrological model is soundly calibrated and tested. Both procedures strongly depend on data availability and quality. Previous investigations within our study area in northern Thailand revealed that contaminants such as pesticides tend to be transported to stream water by lateral subsurface flow (Kahl *et al.*, 2007; Kahl *et al.*, 2008; Duffner *et al.*, 2012; Sangchan *et al.*, 2012). Duffner *et al.* (2012) and Hugenschmidt *et al.* (2010) pointed to a considerable fraction of shallow subsurface flow (i.e. lateral flow) on total flow during single events in a small subcatchment at the site. This finding implies that a model, which is intended to be used to simulate the transport of contaminants, must not only be calibrated with regard to a precise reproduction of the water balance and discharge dynamics but also with a reasonable partitioning of run-off generating flow components.

*Correspondence to: M. A. Bannwarth, Institute of Soil Science and Land Evaluation, Biogeophysics Section, University of Hohenheim, Stuttgart, Germany.
E-mail: bannwart@uni-hohenheim.de

Of the vast number of hydrological models available, only a few are capable of simulating complex land management operations and pesticide transport at catchment scale. One of these models is the Soil and Water Assessment Tool (SWAT; Arnold *et al*., 1998), which has been applied frequently to watersheds worldwide (see Gassman *et al*., 2007). Most SWAT applications have been carried out in temperate regions (i.e. Larose *et al*., 2007; Green and van Griensven, 2008; Holvoet *et al*., 2008; Ullrich and Volk, 2010; Neitsch *et al*., 2011). The number of SWAT model studies carried out in tropical or subtropical regions, however, is increasing (Tripathi *et al*., 2003; Ndomba *et al*., 2008; Schuol *et al*., 2008; Setegn *et al*., 2010; Strauch *et al*., 2012). Nevertheless, most applications focus only on water balance (Table I). This is particularly true for studies conducted in Thailand. Kuntiyawichai *et al*. (2011), for example, performed SWAT simulations to evaluate flood management options in the 4145-km^2 Yang River basin in northeast Thailand. Another SWAT application was carried out by Reungsang *et al*. (2010) in a sub-basin of the 7000-km^2 Chi River. SWAT reproduced the monitored run-off well, but the R^2 never exceeded 0.72. Phomcha *et al*. (2011) simulated discharge in the Lam Shonti watershed (357 km^2) in central Thailand, where the elevation ranges between 100 and 700 m a.s.l. and land use was dominated by forest and agriculture. The SWAT model performed well, but the study demonstrated some shortcomings in predicting stream flow during the dry season. Collectively, none of the SWAT model applications in Thailand have been carried out in catchments with less than 100 km^2 (Table I). Also, catchments with steep orography have not been simulated. Furthermore, none of the studies focused on simulating solute run-off or transport partitioning.

Manual calibration of model parameters is a time-intensive and labour-intensive task that does not necessarily yield the best parameter set. Hence, automatic calibration techniques are widely applied these days. Examples for frequently used automatic calibration techniques are (i) Markov chain Monte Carlo (MC^2) methods, which derive optimal parameters from a large number of runs with different parameter sets (Metropolis *et al*., 1953); (ii) shuffled complex evolution (SCE), which uses an intelligent search algorithm to find the best parameter distribution (Duan *et al*., 1988); and (iii) SUFI2 (sequential uncertainty fitting) which uses the uncertainty bands of MC^2 runs for optimization (Abbaspour *et al*., 2004). Calibration of complex models is hampered by uncertainties in input data as well as by limitations of model structure and parameterization. One complicating issue is often the lack of model flexibility to accurately represent catchment heterogeneity and scale processes. Several techniques have been developed to assess model uncertainties including Bayesian approaches (e.g. Kuczera and Parent, 1998; Ajami *et al*., 2007), autoregressive error models (e.g. Duan *et al*., 1993; Bates and Campbell, 2001) and 'fuzzy' approaches that do not have strict statistical assumptions [e.g. the Generalized Likelihood Uncertainty Estimation (GLUE; Beven and Binley, 1992)].

The built-in automatic calibration functionality in SWAT is performed with Parasol, a method based on SCE algorithm (van Griensven *et al*., 2006). The major drawback of Parasol relates to the electability of model parameters. To save computer time, Parasol reduces the number of parameters by calibrating all parameters of one modelled category together. This lumped approach limits the possibility to parameterize spatially variable processes in a heterogeneous catchment. To overcome this issue, Lin and Radcliffe (2006) first calibrated a set of lumped parameters across a catchment, then coupled SWAT with the PEST parameter estimation software (Doherty and Johnston, 2003), a code for inverse parameter optimization based on the Gauss–Marquardt–Levenberg algorithm, to account for the spatial variability of some elected parameters. Another tool that is used more frequently is SWAT-CUP (Abbaspour *et al*., 2004; http://www.eawag.ch/forschung/siam/software/swat/index), which has evolved into a calibration 'swiss-knife', featuring various calibration methods. However, SWAT-CUP is not drawing a clear line between uncertainty analysis and calibration techniques. GLUE, for instance, is actually a technique to evaluate uncertainty of calibrations and SUFI2 is a hybrid between calibration tool and uncertainty analysis. Its calibration algorithm works by narrowing the uncertainty band around the observations. Therefore, we decided at the beginning of the study to develop our own calibration tool that clearly distinguishes between calibration tool phase and uncertainty analysis. To overcome the calibration problems, which we were faced when trying to find the best parameter set for a heterogeneous watershed, we developed a new optimization tool: ANSELM (A Nash–Sutcliffe Efficiency Likelihood Match). This optimization tool allows assigning parameters to specific soil and land-cover units. In this way, spatial information, which is often lost by lumped calibration approaches, is included in the calibration and thus improves the model efficiency. All SWAT parameters are available for selection, which is not the case in Parasol. The ANSELM tool is easy to handle and does not need an intensive training. Additionally, it provides a GLUE uncertainty analysis of the calibrated simulation results. Last but not least, it can be modified to calibrate any simulation output of SWAT. It can be used, for example, for pesticide load calibration, which will be necessary for us in the future.

In this work, we investigate the applicability of the SWAT model in simulating the discharge dynamics and hydrograph partitioning in a tropical, mountainous headwater catchment. The SWAT model was calibrated and

Table I. Overview of current studies on stream flow calibration with SWAT in Thailand and climatically comparable regions in South-East Asia

Study	Calibration goal	Study site	Elevation (m a.s.l.)	Precipitation	Land use	Number of gauging stations	Simulation period	Model efficiency (stream flow calibration)
Khoi and Suetsugi, 2014	Stream flow, sediment	Be River catchment, 7500 km^2, Central Vietnam	100–1000	2400 mm (May–Oct)	51% agriculture, 43% forest, 6% urban and others	1	10-year calibration	R^2 = n.a. *NSE* = 0.8
Reungsang *et al*., 2010	Stream flow	Chi River, sub-basin II, 7000 km^2, northeast Thailand	148–250	1193 mm (May–Oct)	56% rice, 15% field crops, 10% forest, 6% pasture and 13% urban	4	1-year calibration 3-year validation	R^2 = 0.77–0.88 *NSE* = 0.55–0.79
Kuntiyawichai *et al*., 2011	Stream flow	Yang River, 4145 km^2, sub-basin of Chi River, northeast Thailand	600 m on average	1390 mm (May–Oct)	4% urban, 60% agriculture, 33% forest and 3% water bodies	1	1-year calibration	R^2 and *NSE* > 0.85
Phomcha *et al*., 2011	Stream flow	Lam Shonti catchment, 357 km^2, central Thailand	100–700	1134 mm (May–Oct)	59% forest, 38% agriculture and 3% others	1	2-year calibration 2-year validation	R^2 = 0.895 *NSE* = 0.848
Graiprab *et al*., 2010	Stream flow, climate projections	2 sub-regions of At Samat sub-basin, Chi River, 205 and 438 km^2, northeast Thailand	115–150	1507 mm (May–Oct)	80% agriculture, 7% forest, 4% urban, 9% water and others	2	8-year calibration[a]	R^2 = n.a. *NSE* = 0.7–0.89
Alansi *et al*., 2009	Stream flow forecasting	Upper Bernam River, 1097 km^2, Malaysia	Up to 1830	1800–3500 mm (May–Oct)	3% urban[b], 11% oil palm[b], 23% rubber[b], 54% forest[b] and 2% orchards[b]	1	24-year calibration 3-year validation	R^2 = 0.65–0.82, *NSE* = 0.62–0.81
Alibuyog *et al*., 2009	Stream flow sediment	Kiluya and Kalaignon, sub-basins of Manupali catchment, 2 km^2, Philippines	900–2000	2347 mm (Jun–Oct)	17% forest, 29% agriculture, 53% grassland and 1% footpaths	4	1-year calibration	R^2 = 0.87–0.99 *NSE* = 0.77–0.83

[a] Calibration was adopted from model application by Rossi *et al*. (2009).
[b] Land use is given in averages because it changed within the calibration period.
[c] n.a.: not available data in this study.

tested on a 3-year dataset with ANSELM. The results were compared with the outcome of a Parasol calibration. The performance of the calibrated model is assessed with different efficiency criteria and with the help of an uncertainty analysis. Finally, the composition of the simulated stream flow is evaluated in detail.

MATERIAL AND METHODS

Study site

The Mae Sa catchment (18°54′N, 98°54′E) is located 35 km north-west of Chiang Mai in northern Thailand (Figure 1). The catchment has a total area of 77 km^2 spread over elevations ranging from 325 to 1540 m a.s.l. Sharp relief and narrow valleys dominate the catchment. The mean slope is 36%, but slopes steeper than 100% are abundant. The Mae Sa River is a tributary of the Ping River, one of the major rivers in northern Thailand draining to the Chao Phraya. The river has a length of 12 km; and bed slope ranges between 1% and 20% (mean = 5%). About 24% of the catchment area is devoted to agriculture. The remaining area is mostly covered by deciduous and evergreen forests of varying degrees of disturbance. Acrisols and Cambisols are the main soil types within the catchment (Schuler, 2008). Mean air temperature is 21 °C, and annual rainfall is 1250 mm on average (2004–2010). The tropical climate in the area is dominated by a rainy season stretching from May to late October, followed by a lengthy dry season (November to April).

Monitoring programme and data analysis

Discharge, rainfall and general meteorological variables were monitored in the Mae Sa catchment from July 2007 to December 2010. Solar radiation, rain, air temperature, relative humidity and wind speed (Thies, Germany; UIT, Germany) were measured at two automated climate stations. Additionally, rainfall was recorded by 12 automatic tipping bucket gauges (Fischer GmbH, Germany) (Figure 1). Discharge of the Mae Sa River was monitored at the main catchment outlet at 10-min intervals by an ultrasonic water level sensor (710 Ultrasonic module, Teledyne ISCO Inc., USA). Hand measurements of discharge for establishing the stage-discharge calibration curve were conducted with an acoustic digital current metre (Model ADC, OTT ADC GmbH, Germany) at a broad range of flows. Discharge measurements at the outlet were evaluated against data from another gauging station located 3 km upstream (Ziegler *et al*., submitted).

The SWAT model

SWAT is a semi-distributed hydrological model performing on a daily time step. SWAT divides a catchment into sub-basins that are each subject to different micro-climatic forcing. Each sub-basin is further partitioned into a number of Hydrological Response Units (HRUs) that

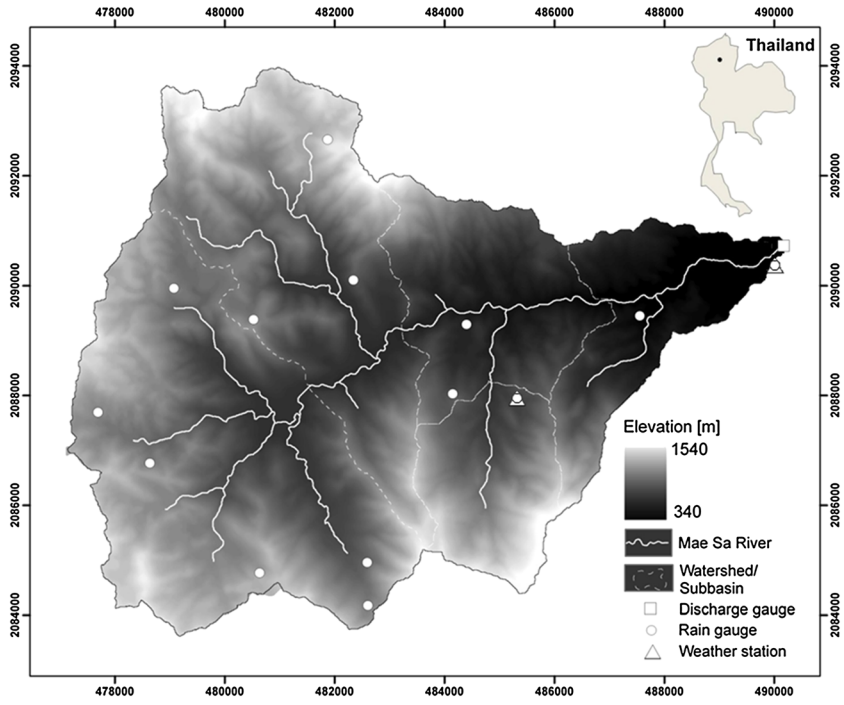

Figure 1. Topographic map of the Mae Sa watershed, position of monitoring stations and the five sub-basins used in the SWAT model

represent various combinations of land use, soil type and relief. A water budget is computed for each HRU on the basis of evapotranspiration, precipitation, run-off, percolation and return flow from groundwater and subsurface flow (Neitsch *et al.*, 2011):

$$SW_t = SW_0 + \sum_{i=1}^{t} \left(R_i - Q_{\text{surf},i} - E_{a,i} - w_{\text{seep},i} - Q_{gw,i}\right) \quad (1)$$

where SW_t (mm) is the soil water content at day t, SW_0 (mm) stands for initial soil water content, R_i (mm) denotes rainfall depth, $Q_{\text{surf},i}$ (mm) is surface run-off, $E_{a,i}$ (mm) is evapotranspiration, $w_{\text{seep},i}$ (mm) is the water entering the vadose zone from the soil profile and $Q_{gw,i}$ (mm) is the amount of base flow. In all cases, the subscript i denotes the i-th preceding day.

Setup of the SWAT model and sensitivity analysis

The Mae Sa catchment was divided into five sub-basins for simulating discharge generation at a daily time step (Figure 1). Preliminary testing suggested that finer sub-basin division did not significantly improve simulation results but greatly increased computing time. One rain gauge was selected to represent each sub-basin (Figure 1). Data from the remaining nine rain gauges within the Mae Sa catchment were used to fill gaps caused by technical failures. Soil input data were based on prior field work (Schuler, 2008). Elevation and land use were derived from a SPOT 5 image (November 2006; scene centre = N19°1′4″ E98°49′24″), provided by the Geo-Informatics and Space Technology Agency (GISTDA, 2007). Parameters for forest vegetation were manually altered from model default values (SWAT2009.mdb; Ver. 2009/Rev481) to align with those of tropical vegetation in the catchment (e.g. increasing maximum of total biomass, LAI and heat units to maturity). Input on management operations were based on interviews with local farmers (Schreinemachers *et al.*, 2011). The spatial range of all parameters is given in Table II; concerning groundwater parameters, there were no on-site data available, so for model setup, we used expert guesses. Following an initial parameterization, a sensitivity analysis was performed with a Latin-hypercube approach (van Griensven *et al.*, 2006; van Griensven and Meixner, 2007) to identify the ten most sensitive parameters to be used in the subsequent calibration.

Model calibration

Parasol with SCE searches a global optimum in the parameter space based on the sum of squared residuals (SSQ) or a ranked version of SSQ. Parameters can be updated during the calibration only by assigning new values or adjusting via scalar addition or multiplication (Figure 2), either for the whole catchment or for a predefined selection of HRUs. It is not possible to calibrate parameters for specific soil, slope or land-cover units simultaneously. For example, let us assume that the user wishes to estimate the saturated hydraulic conductivity in a catchment, which has been separated into six HRUs, where HRUs 1, 2 and 4 contain soil profile 1, HRU 3 contains soil profile 2 and HRUs 5 and 6 contain soil profile 3. The user can choose (i) whether one single conductivity value is calibrated for

Table II. Ranking, calibration range and initial values of the ten most sensitive parameters used in calibration of the SWAT model

Parameter	Rank	Description	Unit	N_HRU[a]	Calibration range[b]	Initial value
Rchrg_Dp	1	Deep aquifer percolation fraction	—	5	0–1	0.05
Gwqmn	2	Threshold depth of water in the shallow aquifer required for return flow to occur	mm	5	0–1000	100
GW_Delay	3	Groundwater delay	days	5	0–200	31
Sol_K	4	Saturated hydraulic conductivity (K_s)	mm/h	2	0–100	10–23
CN_2	5	Run-off curve number	—	4	30–95	55–77
Slope	6	Average slope steepness	m/m	5	0–0.99	0.02–0.6
Sol_Awc	7	Available soil water capacity	1	2	0.01–0.5	0.13–0.18
Esco	8	Soil evaporation compensation factor	—	4	0–1	0.9
Alpha_Bf	9	Base flow alpha factor, or recession constant	—	5	0–1	0.048
Slsubbsn	10	Average slope length	m	5	0–200	10–120

[a] Number of different HRU classes. A parameter was simultaneously calibrated for five slope classes, two soil classes or four land-use classes.
[b] The range depicts parameter values for different HRU classes.

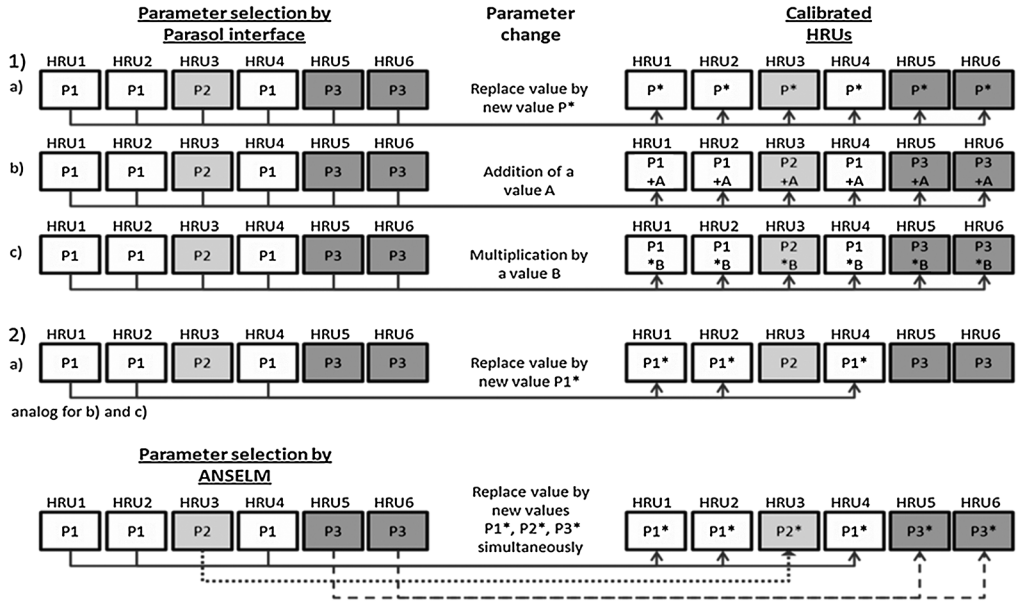

Figure 2. Schematic overview of the two calibration tools over six HRUs. PX is related to calibration class X, $X = 1,\ldots,6$ (e.g. the average slope value 1 to the slope class 1)

all HRUs, (ii) whether a constant added to the default values is calibrated or (iii) whether a constant factor of the default values is calibrated. Parasol does not allow calibrating a parameter separately for different HRU classes (unlike ANSELM, Figure 2).

This approach severely limits the possibilities to represent the spatially variable properties of a catchment. Furthermore, not all parameters can be calibrated.

ANSELM, which is written in Matlab (Version 7.10.0, http://www.mathworks.de), uses the Nash–Sutcliffe efficiency (NSE; Nash and Sutcliffe, 1970) as objective function during calibration. It can simultaneously modify values of all parameters separately for different HRU classes. Any SWAT input parameter can be calibrated. ANSELM uses a MC^2-calibration approach. It applies a triangular probability density function (pdf) within predefined ranges. Range and peak value of the pdf are derived by expert guesses or measurements; the pdf decreases from the peak value linearly to zero at the upper and lower borders of the range.

Model calibration was performed with the 2008 Mae Sa daily time series data. In the first calibration approach using Parasol, the ten most sensitive parameters derived from the sensitivity analysis were selected. As initial values, we used the values of the SWAT model setup. Where applicable, the ranges were set according to single on-site measurements, otherwise according to the default ArcSWAT interface with physically meaningful values (Table II). The maximum number of optimization simulations was limited to 70 000. This procedure was applied analogously to the top ten high-leverage parameters.

Besides the objective functions used during calibration – that is, the NSE and a normalized sum of squared residuals (nSSQ) – we further applied the Kling–Gupta efficiency (KGE; Gupta *et al.*, 2009) for model evaluation. The equations are

$$NSE = 1 - \frac{\sum_{t=1}^{n} \left(q_o^t - q_s^t\right)^2}{\sum_{t=1}^{n} \left(q_o^t - \overline{q}_o\right)^2} \tag{2}$$

$$nSSQ = \frac{1}{n} \sum_{t=1}^{n} \left(q_o^t - q_s^t\right)^2 \tag{3}$$

$$KGE = 1 - \sqrt{(r-1)^2 + (\alpha - 1)^2 + (\beta - 1)^2} \tag{4}$$

with $\alpha = \sigma_s / \sigma_o$ and $\beta = \overline{q}_s / \overline{q}_o$

where q_o^t and q_s^t ($m^3\,s^{-1}$) are observed and simulated discharge at time t, respectively. The symbols $\overline{q}_o$ and $\overline{q}_s$ (m^3/s^{-1}) stand for mean observed and simulated discharge, respectively. The symbols σ_s and σ_o are the standard deviations of the simulated and observed discharge; and $\boldsymbol{r}$ denotes the linear correlation coefficient between the simulated and observed values. The index $\boldsymbol{n}$ is the number of time steps. The NSE and KGE indices range from $-\infty$ to 1, where 1 denotes the best model efficiency. The nSSQ ranges from 0 to ∞, where ∞ denotes the best efficiency.

Uncertainty analysis

ANSELM employs a GLUE uncertainty analysis approach (Beven and Binley, 1992) based on the following weighted likelihood equation:

$$w_i = \frac{NSE(i)}{\sum_{j=1}^{N} NSE(j)} \quad (5)$$

where w_i is the weight of the i-th behavioural run. A run is set as 'behavioural' when its respective likelihood function (in this case the NSE) is above a certain threshold predefined by the user. The symbols $NSE(i)$ and $NSE(j)$ denote the NSE of the i-th and j-th behavioural runs, respectively; and N is the number of behavioural runs. The 95% prediction uncertainty (PU) bands for daily discharge are derived from the cumulative density function of all weighted behavioural runs. The NSE was taken as the likelihood function, and the threshold for non-behavioural runs was set to zero. The zero value was chosen to obtain broad uncertainty bands that should cover all of our observations. This choice is in line with other GLUE applications using SWAT (Yang *et al.*, 2008; Shen *et al.*, 2012).

The uncertainty analysis in the Parasol calibration follows the approach of van Griensven and Meixner (2007). The method, based on χ^2 statistics (Bard, 1974), divides the sample population in simulations with 'good' and 'bad' parameter sets. The SCE finds a parameter set consisting of p free parameters with lowest SSQ. The threshold of a 'good' set is defined by the equation

$$c = SSQ(\theta^*) \cdot \left(1 + \frac{\chi^2_{P,0.95}}{N - P}\right) \quad (6)$$

where N stands for the number of observations, θ^* denotes the vector with the best parameter values and $\chi^2_{P,0.95}$ is χ^2 for P parameters at a 95% confidence level. The 95% PU bands of daily discharge are derived from the highest and lowest daily values of all 'good' simulations.

RESULTS

Model calibration and validation

Of the 27 parameters selected by the Latin-hypercube sensitivity tool for discharge optimization, the three most sensitive were those associated with simulating base flow: Rchrg_Dp, Gwqmn and Gw_Delay (Table II). The next most sensitive parameters were the soil parameter Sol_K, which controls water flux in soil and curve number (CN_2), which governs infiltration and thereby surface run-off generation. The only sensitive parameter related to evaporation was Esco, which controls the loss of water by evapotranspiration from deep soil layers. The final calibrated parameter values using Parasol (Parasol-SWAT) and ANSELM (ANSELM-SWAT) are shown in Table III. The spatial variability of the calibrated parameters, by way of example, is shown in Figure 3 for Gwqmn. The distribution pattern follows mostly the distribution of the slope classes. Values of Gwqmn are low in the valley and high on steeper slopes, which means that in the valley, base flow is initiated from the shallow aquifer at lower water levels than on hill slope positions.

The model efficiencies of the simulations of the calibration year (2008) and the validation years (2009 and 2010) are shown in Table IV. The simulations were performed with the parameters derived from the final run of both calibration methods respectively. ANSELM-SWAT yielded the best simulation result for the 2008 calibration period: NSE, nSSQ and KGE values were 0.83, 0.07 and 0.81, respectively. In the first test period (2009), modelling efficiencies only slightly dropped ($NSE = 0.77$). In contrast, the NSE of Parasol-SWAT significantly decreased from

Table III. Calibrated parameter values of the two calibration approaches

Parameter[a]	Unit	Parasol	ANSELM[b]
Rchrg_Dp	—	0.22	0.11–0.253
Gwqmn	mm	335.99	98.12–350.67
GW_Delay	days	186.16	24.56–74.35
Sol_K	mm/h	43.18	9.56–27.45
CN_2	—	53.98	36.59–66.52
Slope	m/m	0.26	0.047–0.658
Sol_Awc	mm/mm	0.5	0.12–0.2
Esco	—	0.28	0.26–0.43
Alpha_Bf	—	0.149	0.009–0.11
Slsubbsn	m	105.25	12.00–112.11

[a] Parameter descriptions are listed in Table II.
[b] The range depicts parameter values of different HRU classes.

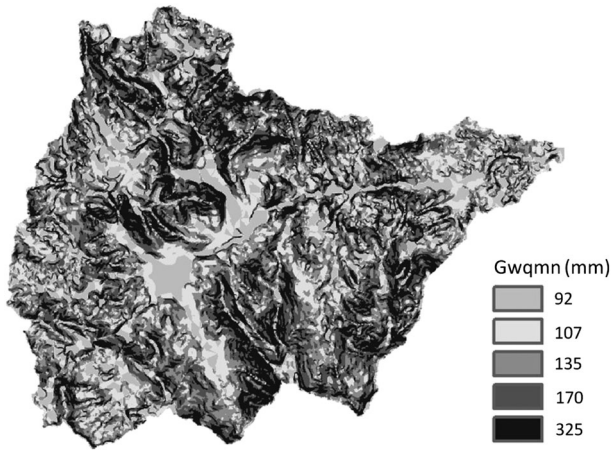

Figure 3. Spatial distribution of the Gwqmn parameter within the Mae Sa watershed after calibration [Gwqmn: water in the shallow aquifer required for return flow to occur (mm)]

Table IV. Performance of the SWAT model after the optimization with Parasol and ANSELM

	Parasol			ANSELM		
Year	NSE	nSSQ	KGE	NSE	nSSQ	KGE
2008[a]	0.62	0.17	0.80	0.83	0.07	0.81
Dry season	0.83	0.06	0.86	0.93	0.02	0.82
Rainy season	0.47	0.27	0.67	0.76	0.12	0.79
2009[c]	0.23	0.26	0.52	0.77	0.08	0.82
Dry season	0.27	0.09	0.51	0.89	0.01	0.71
Rainy season	0.21	0.46	0.54	0.73	0.14	0.84
2010[c]	0.66	0.53	0.53	0.87	0.20	0.83
Dry season	0.36	0.20	0.52	0.90	0.03	0.76
Rainy season	0.70	0.87	0.54	0.86	0.36	0.85

[a] Calibration year.
[b] Validation year.
NSE, Nash–Sutcliff efficiency; nSSQ, normalized sum of squared residuals; KGE, Kling–Gupta efficiency. Values are for the best runs of the three calibration approaches.

0.62 in the 2008 calibration simulation to 0.23 during the 2009 test simulation. In the second validation period (2010), the NSE values of both methods were higher than in the calibration year (0.66 and 0.87 for Parasol and ANSLEM, respectively). The better performance in 2010 is related to the fact that the NSE objective function weights are proportional to peak magnitudes. High peaks at the end of 2010 inflated the NSE of both calibration approaches (Figure 4). In comparison, the sum of squared residuals [Equation (3)] is lowest in 2008 and highest in 2010: for example, with Parasol-SWAT, it increases from 6 to 192, whereas with ANSELM-SWAT, it increases from 27 to 70.

Discharge dynamics

The discharge in the dry periods before and after the rainy season is well captured by ANSELM-SWAT in 2008 and 2010 (Figure 4, Table IV); however, in 2009, ANSELM-SWAT simulates small discharge peaks in February and March that were not observed at the gauging station (Figure 4). The recession behaviour of the hydrograph is well described by ANSELM-SWAT. In comparison, Parasol-SWAT shows severe deficiencies in predicting the recession limbs at the end of the rainy season. Flashy discharge during the rainy season is generally well reproduced by ANSELM-SWAT (Figure 4). Parasol-SWAT simulations match the observations at the end of the dry season (January to April, Table IV), but they do not perform well at the onset of the rainy season (May to July). The magnitude and recession of discharge peaks markedly deviate from the measured discharge time series. In general, discharge peaks are underestimated, and recessions occur too slowly in both the calibration and validation periods. At best, Parasol-SWAT only captures the 'average' trend of observed discharge in the rainy season.

Annual rainfall did not vary greatly for the 3 years considered (1281–1352 mm; Table V). However, annual discharge was greatly different in 2008 and 2009 compared with 2010 (378–423 *vs* 517 mm; Table V). The 2010 rainy season commenced almost 4 weeks later than in the two previous years but received the same total amount of rainfall. Several large storms produced larger discharge peaks in 2010 compared with the previous years. Both calibration approaches closely matched the observed 2008 annual discharge (378 mm). For 2009, ANSELM-SWAT

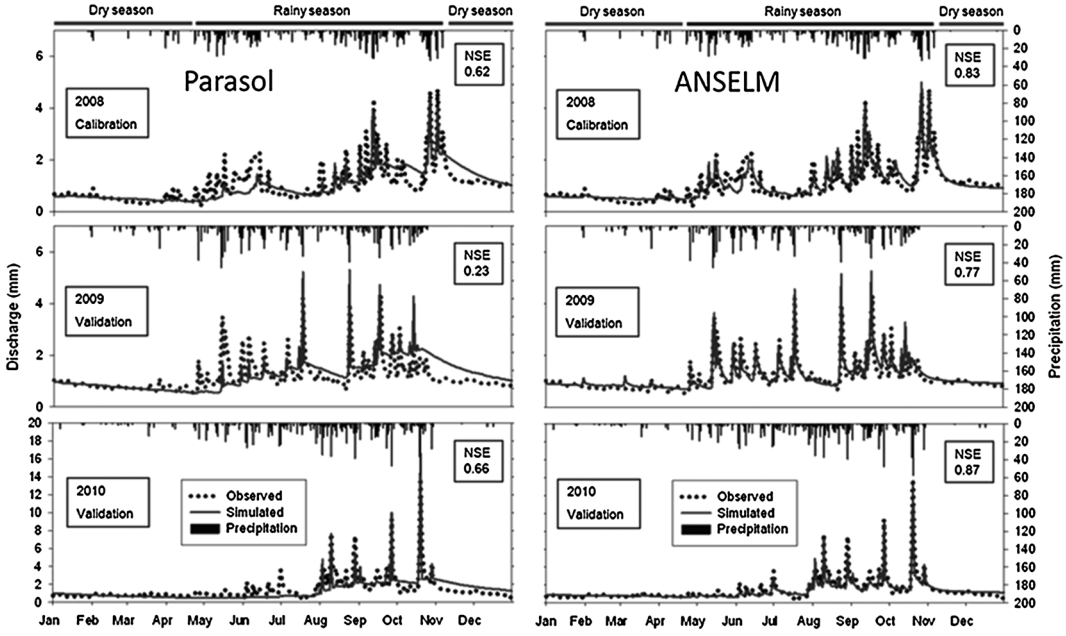

Figure 4. Observed and simulated discharge at the outlet of the Mae Sa watershed together with the corresponding precipitation. Left: Final calibration using the Parasol method. Right: Final calibration using the ANSELM method. Note the different scale of the discharge axis in 2010

Table V. Observed and predicted total annual discharge of the two calibration approaches

Year	Annual discharge (mm)			Annual run-off coefficient	Annual run-off coefficient	Observed annual precipitation (mm)
	Parasol	ANSELM	Observed	ANSELM	Observed	
2008	371	382	378	0.28	0.28	1352
2009	456	432	423	0.34	0.33	1281
2010	492	496	517	0.37	0.39	1316

and Parasol-SWAT slightly overestimated the annual discharge (423 mm) by 2% and 8%, respectively. In 2010, both methods underestimated the annual discharge (517 mm) by 5% (Parasol-SWAT) and 4% (ANSELM-SWAT). The predicted run-off coefficients (ROCs) based on the ANSELM-SWAT simulations were very similar to the observed ROCs (Table V).

Time series uncertainty analysis

The 95% PU bands of the Parasol calibration were generally narrower than those derived by the GLUE analysis with ANSELM (Figure 5). Consequently, observed discharge values frequently fell outside the confidence bands of Parasol. Only seven out of 70 000 Parasol model runs were identified as 'good', on the basis of the threshold Parasol used (2.7). The ANSELM approach produced nearly 45 000 runs that were behavioural. The observed time series falls completely within the PU band from the ANSELM simulations. Nevertheless, ANSELM-SWAT does tend to underestimate the base flow in some simulations during the dry season, because the observations are mostly on the upper edge of a broad uncertainty band from December to May (Figure 5). Uncertainty in predicting rainfall event peaks increases proportionally with the peak magnitude, the uncertainty band is much broader, when huge discharge peaks are simulated.

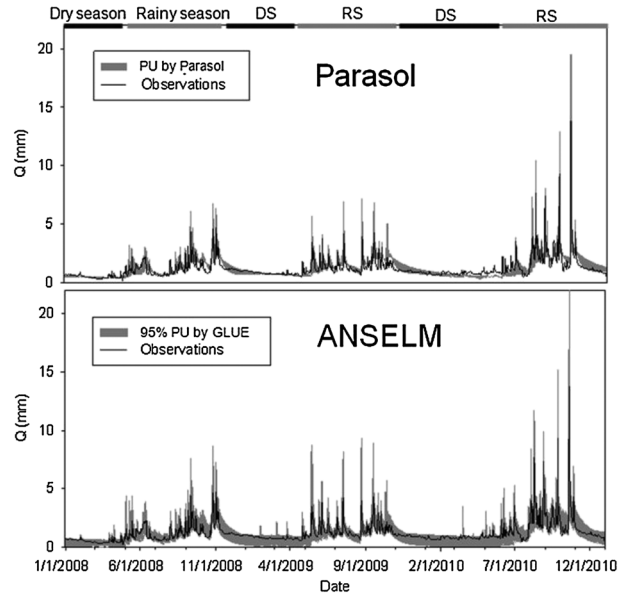

Figure 5. Predicted uncertainty bands of the daily discharge for the years 2008 to 2010 for both calibration approaches based on the calibration period 2008

Simulating flow components

Although observed hydrological conditions were highly variable in time, the dynamics of the discharge was reproduced well during all periods by ANSELM-SWAT (Figure 4). Parasol-SWAT, however, was not suited for simulating all flow components. For example, the poorly reproduced recession limbs indicated that lateral flow was not simulated accurately. Because the ANSELM approach yielded the highest values of all objective functions (Table IV), its final parameter set was chosen to evaluate the different flow components contributing to the total discharge (Figures 6 and 7). Despite the given temporal differences between the study years (Figure 6), some general flow component trends were observed in all years. Base flow contributed almost 100% to the stream flow in the very dry period between December and March. The base flow fraction increased throughout the rainy season with a high near the end of the year. In the second dry period after the rainy season, the contribution of base flow increases from year to year (Figure 5; 2008: from 0.6 to 0.85 mm/day; 2009: from 0.85 to 0.93 mm/day; and 2010: 0.93 to 1.0 mm/day).

Only substantial basin-wide rainfall contributions would trigger small peaks of surface run-off and lateral flow in the beginning of a year (Figures 6 and 7). Then, at the beginning of the wet season as rainfall occurred more frequently, the total stream flow was influenced by both base flow and lateral flow (as indicated by the near parallel component hydrographs in Figures 6 and 7). The volume of lateral flow produced during storms increased after the onset of the rainy season (Figure 6). This behaviour is interrupted by surface run-off peaks, which evolve almost directly at the time of the respective rain event. The magnitude of the peak was controlled by the amount of rainfall when the rain event occurred. In the beginning of the rainy season, rain events produced only small surface run-off peaks. In comparison, events at the end of the rainy season often generated very high peaks (e.g. October 2010; Figures 5, 6C and 7C). These

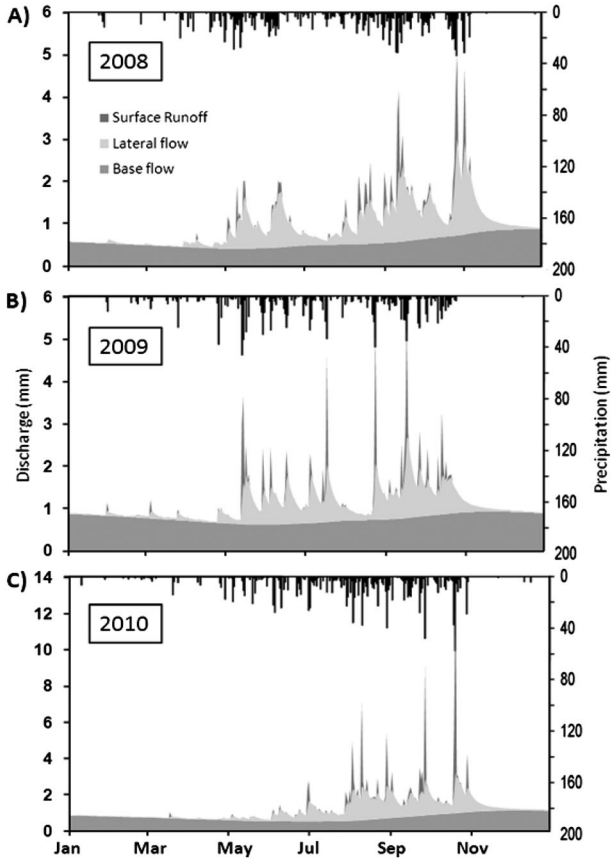

Figure 6. Simulation of the flow components by SWAT based on the final ANSELM calibration. Flow components are depicted on top of each other, the upper horizon equals the total discharge

high surface run-off peaks dominated storm discharge response. For example, surface run-off contributed 75% of the largest stream discharge peak in late October 2010. Throughout the year, the shapes of the recession limbs of the lateral flow and total stream flow were similar (Figures 5 and 6D).

DISCUSSION

Applicability of ANSELM

Both calibration approaches yielded acceptable model efficiencies after 70 000 optimization steps, while Parasol needed approximately 2 h longer (4% of the total time ANSELM needed). The ANSELM tool, however, identified already first acceptable parameter sets (i.e. produce NSE of >0.5; Moriasi *et al.*, 2007) after less than 100 optimization steps. In contrast, the Parasol calibration approach required more than 45 000 optimization steps to obtain first simulations with an NSE above 0.5. The performance differences could relate to the different search algorithms. Also the lower final model efficiencies could be attributed to this difference in the parameterization set. In summary, the ANSELM-SWAT coupling proved to be a useful method to calibrate the SWAT model for simulating hydrological response in a steep mountainous tropical catchment.

Discharge simulations

SWAT simulated reasonably both magnitude and timing of discharge peaks in 2008 and 2010. The closeness of simulated and observed stream flow in the dry season and the reasonably pictured base flow recessions suggest that the parameters controlling the base flow conditions, such as Gwqmn, Rchrg_Dp, GW_Delay and Alpha_Bf, were well estimated. This statement is further supported by the finding that the simulation of discharge during dry season performed better than during the rainy season (Table IV). Our finding that the mean slope parameter of every HRU is the sixth most sensitive parameter demonstrates the importance of topography in SWAT. Hugenschmidt *et al.* (2010) and Duffner *et al.* (2012) used dissolved silica as tracers to perform a three-component hydrograph separation in a subcatchment of the Mae Sa watershed. Taking their results into account, the simulation of the different flow components showed a reasonable partitioning of surface run-off, lateral flow and base flow. Over the whole simulation period, base flow (i.e. groundwater) contributed fractions of 64% of the whole annual discharge (Duffner *et al.* 2012: 80–96%). Lateral flow delivered 29% (Duffner *et al.*, 2012: 3–18%), and surface run-off was at 7% (Duffner *et al.*, 2012: 1–7%). The fraction of each flow component varied among the season (Table VI). The direct flow components, surface run-off and lateral flow, were low during the dry season but significantly increased in the rainy season.

Discrepancies of measured *versus* simulated discharge peaks are most probably related to the steep topography and narrow valleys that cause the flashy hydrograph behaviour of Mae Sa catchment. Limited flood plain areas in the upper portion of the catchment likely result in fast routing of storm flow to the stream. Also, the geometry and the similar length of the tributaries in the upper part of the catchment support a fast response (Figure 1). The relatively equal flow path length from the catchment boundary to each tributary may cause a sudden response and an overlay of the run-off response at the observation point. Some experimental studies on various scales and from different tropical environments may lend insight into the reliability of our simulation results. Dykes and Thornes (2000) reported that overland flow rarely occurred during their studies in a steep tropical rainforest catchment in Brunei. The small contribution of annual surface run-off (7%; Table VI) computed in the simulations is reasonable because more than 70% of the catchment is covered by forest. They also identified storm flow run-off coefficients of about 0.4. The annual run-off coefficients simulated by ANSELM-SWAT range between 0.28 and 0.37 (Table V). Although this number is quite low compared with the storm flow run-off coefficients mentioned earlier, it is still in reasonable range,

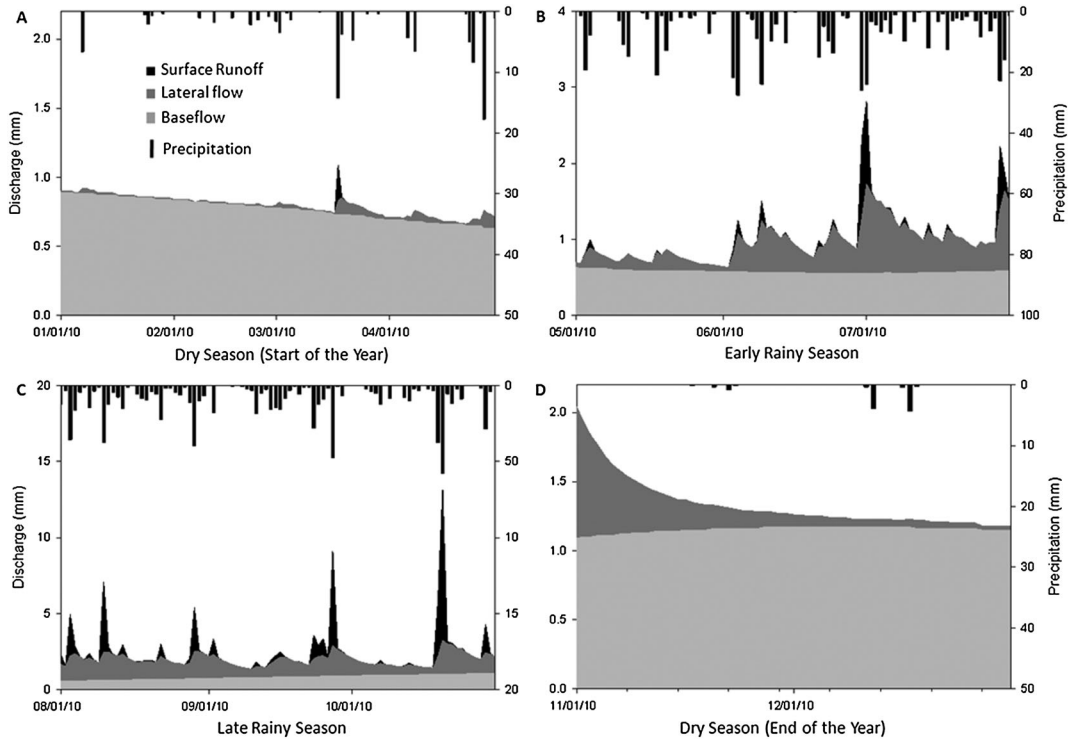

Figure 7. Simulation of the flow components with ANSELM-SWAT for four characteristic periods exemplified for the year 2010. Flow components are depicted on top of each other. The upper line equals the total discharge

Table VI. Mean contribution of the three major flow components to stream flow as simulated using parameter sets identified by Parasol and ANSELM approaches

Flow component (%)	Parasol	ANSELM		
	Complete season	Complete season	Rainy season	Dry season
Surface run-off	6.5	7.3	11.1	0.9
Lateral flow	29.7	28.8	45.2	11.7
Base flow	63.8	63.9	43.8	87.5

The values cover the total observation period from 2008 to 2010.

because it represents the average over the rainy and dry seasons. Base flow dominates the hydrograph during the dry season but is overwhelmed by lateral flow during the rainy season. Lateral flow – in varying nomenclature – is considered to be dominant or at least important in tropical storm flow generation (i.e. Giertz *et al*., 2006; Ziegler *et al*., 2007; Wickel *et al*., 2008). Hence, the simulation of higher fractions of lateral flow during the rainy season is in agreement with field observations.

Depletion of soil water after the end of the rainy season is adequately represented by the recession of the lateral flow (Figures 6 and 7D). At this time, base flow is again the dominant stream flow component, sustaining the discharge during the extended period of low rainfall. This stable behaviour in hydrological response favours a reasonable fit of the calibration parameters, which allows the use of the model for further specific applications, where a reliable separation of flow components is needed.

Although rainfall during all years did not differ greatly, run-off was substantially higher towards the end of the rainy season in 2010. This response was probably caused by the fact that the same precipitation amount was concentrated on a shorter period in 2010, which led to higher storm intensities causing different catchment wettings. The difference in run-off among those years is simulated adequately by SWAT, providing additional evidence for reasonable parameterization of the model. The use of different uncertainty methods by Parasol and ANSELM (χ^2 and GLUE) results in different widths of the confidence bands. Compared with the band generated by the GLUE method, the band generated by χ^2 is so narrow that it does not cover the observations. Furthermore, the χ^2 method covers the parameter uncertainty, whereas the GLUE method covers all sources of uncertainty (Beven and Binley, 1992; Beven and Freer, 2001).

Comparison of model performance with other studies

On the basis of the default model parameterization, SWAT was not able to simulate the observed hydrograph adequately. Critical parameters related to run-off generation (e.g. curve number) and topography were not well matching the tropical, mountainous conditions of the Mae Sa

catchment. In addition, base flow-related parameters were very sensitive in this catchment, where long dry periods cover nearly half of the modelling period. Following an extensive parameter optimization, SWAT optimized with ANSELM reached high NSEs ($NSE = 0.77–0.87$), which transcends the model performance of other SWAT studies under similar climatic conditions.

A comparison with the following studies is justified because they show similar climatic properties. Tripathi *et al*. (2003) reported for their monsoon-driven, North Indian catchment that discharge peaks were underestimated in the beginning of the study period and then overestimated during later periods. Phomcha *et al*. (2011) produced results for their site in central Thailand that were congruent with those reported herein: NSE values >0.7 were achieved during both calibration and testing periods. Elsewhere, Reungsang *et al*. (2010) reported R^2 values of ≤0.72 for their simulations in a 7000-km^2 sub-basin of the Chi River in Thailand. And recently, Kuntiyawichai *et al*. (2011) achieved an NSE as high as 0.85, and they stated that there was also no clear trend in discrepancies between observed and simulated discharge. The aforementioned studies and further available SWAT applications for South-East Asia (Table I) confirm that the model performance obtained within the present study was in the upper range or even higher than those reported elsewhere both for temperate and tropical zones.

CONCLUSION AND OUTLOOK

The SWAT model was found to be capable of simulating discharge in the 77-km^2 tropical Mae Sa catchment in Thailand at a level of skill equal to or higher than achieved in other catchments worldwide. Part of this success can be attributed to the introduction of the ANSELM tool that allowed assigning unique parameters to specific soil and land-cover units, and thereby leading to a better representation of heterogeneous catchment variables that affect run-off generation. The most sensitive parameters included three related to base flow generation, as well as others that controlled surface flow generation, run-off routing and soil moisture dynamics. The calibrated SWAT model produced good simulations of the timing and peaks of rainy season storm events. Simulation of the base flow in the protracted monsoon dry season was more challenging, yet acceptable. Comparison with results from field experiments in other tropical study sites gives confidence that the separation of the flow components (base flow, lateral subsurface flow and run-off) over all the seasons is reasonable. Hence, simulations for which the partition of the hydrograph becomes relevant are highly possible. In our case, this initial model evaluation phase provides us with confidence that SWAT, coupled with ANSLEM for calibration, can be applied to intended future simulations of pesticide transport in the catchment.

ACKNOWLEDGEMENTS

This project was supported by Deutsche Forschungsgesellschaft (DFG) in the framework of SFB 564 'The Uplands Program' and in part by SARCS grant 95/01/CW-005; APN grants #ARCP2006-06NMY, #ARCP2007-01CMY and #ARCP2007-01CMY; NASA grant NNG04GH59G; and NUS grant R-109-000-092-133. The authors would like to express their gratitude to Dipl.-Math. Anselm Rohland for supporting the development of the ANSELM tool.

REFERENCES

Abbaspour K, Johnson C, van Genuchten M. 2004. Estimating uncertain flow and transport parameters using a sequential uncertainty fitting procedure. *Vadose Zone Journal* **3**: 1340–1352.

Ajami NK, Duan Q, Sorooshian S. 2007. An integrated hydrologic Bayesian multimodel combination framework: confronting input, parameter, and model structural uncertainty in hydrologic prediction. *Water Resources Research* **43**(1), doi: 10.1029/2005WR004745

Alansi A, Amin M, Halim A, Shafri H, Aimrun W. 2009. Validation of SWAT model for stream flow simulation and forecasting in Upper Bernam humid tropical river basin, Malaysia. *Hydrology and Earth System Sciences Discussions* **6**: 7581–7609.

Alibuyog N, Ella V, Reyes M, Srinivasan G, Heatwole C, Dillaha T. 2009. Predicting the effects of land use on runoff and sediment yield in selected sub-watersheds of the Manupali River using the ArcSWAT model. Soil and Water Assessment Tool (SWAT) – Global Applications, World Association of Soil and Water Conservation.

Arnold JG, Srinivasan R, Muttiah RS, Williams JR. 1998. Large area hydrologic modeling and assessment – part 1: model development. *Journal of the American Water Resources Association* **34**: 73–89.

Bard Y. 1974. *Parameter Estimation*. Academic Press: New York.

Bates BC, Campbell EP. 2001. A Markov chain Monte Carlo scheme for parameter estimation and inference in conceptual rainfall-runoff modeling. *Water Resources Research* **37**: 937–947.

Beven K, Binley A. 1992. The future of distributed models – model calibration and uncertainty prediction. *Hydrological Processes* **6**: 279–298.

Beven K, Freer J. 2001. Equifinality, data assimilation, and uncertainty estimation in mechanistic modelling of complex environmental systems using the GLUE methodology. *Journal of Hydrology* **249**: 11–29.

Bruun TB, de Neergaard A, Lawrence D, Ziegler AD. 2009. Environmental consequences of the demise in swidden cultivation in Southeast Asia: carbon storage and soil quality. *Human Ecology* **37**: 375–388.

Doherty J, Johnston JM. 2003. Methodologies for calibration and predictive analysis of a watershed model. *Journal of the American Water Resources Association* **39**: 251–265.

Duan Q, Sorooshian S, Ibbitt RP. 1988. A maximum likelihood criterion for use with data collected at unequal time intervals. *Water Resources Research* **24**: 1163–1173.

Duan QY, Gupta VK, Sorooshian S. 1993. Shuffled complex evolution approach for effective and efficient global minimization. *Journal of Optimization Theory and Applications* **76**: 501–521.

Duffner A, Ingwersen J, Hugenschmidt C, Streck T. 2012. Pesticide transport pathways from a sloped litchi orchard to an adjacent tropical stream as identified by hydrograph separation. *Journal of Environmental Quality* **41**: 1315–1323.

Dykes AP, Thornes JB. 2000. Hillslope hydrology in tropical rainforest steeplands in Brunei. *Hydrological Processes* **14**: 215–235.

Gassman PW, Reyes MR, Green CH, Arnold JG. 2007. The soil and water assessment tool: historical development, applications, and future research directions. *Transactions of the Asabe* **50**: 1211–1250.

Giertz S, Diekkrüger B, Steup G. 2006. Physically-based modelling of hydrological processes in a tropical headwater catchment (West Africa) – process representation and multi-criteria validation. *Hydrology and Earth System Sciences* **10**: 829–847.

Graiprab P, Pongput K, Tangtham N, Gassman PW. 2010. Hydrologic evaluation and effect of climate change on the at Samat watershed, Northeastern Region, Thailand. *International Agricultural Engineering Journal* **19**: 12–22.

Green CH, van Griensven A. 2008. Autocalibration in hydrologic modeling: using SWAT2005 in small-scale watersheds. *Environmental Modelling & Software* **23**: 422–434.

Gupta HV, Kling H, Yilmaz KK, Martinez GF. 2009. Decomposition of the mean squared error and NSE performance criteria: implications for improving hydrological modelling. *Journal of Hydrology* **377**: 80–91.

Holvoet K, van Griensven A, Gevaert V, Seuntjens P, Vanrolleghem PA. 2008. Modifications to the SWAT code for modelling direct pesticide losses. *Environmental Modelling & Software* **23**: 72–81.

Hugenschmidt C, Ingwersen J, Sangchan W, Sukvanachaikul Y, Uhlenbrook S, Streck T. 2010. Hydrochemical analysis of stream water in a tropical, mountainous headwater catchment in northern Thailand. Hydrology and Earth System Sciences Discussion MS No.: hess-2010-65.

Kahl G, Ingwersen J, Nutniyom P, Totrakool S, Pansombat K, Thavornyutikarn P, Streck T, 2007. Micro-trench experiments on interflow and lateral pesticide transport in a sloped soil in northern Thailand. *Journal of Environmental Quality* **36**: 1205–1216.

Kahl G, Ingwersen J, Nutniyom P, Totrakool S, Pansombat K, Thavornyutikarn P, Streck T. 2008. Loss of pesticides from a litchi orchard to an adjacent stream in northern Thailand. *European Journal of Soil Science* **59**: 71–81.

Khoi DN, Suetsugi T. 2014. The responses of hydrological processes and sediment yield to land-use and climate change in the Be River Catchment, Vietnam. *Hydrological Processes* **28**(3): 640–652.

Kuczera G, Parent E. 1998. Monte Carlo assessment of parameter uncertainty in conceptual catchment models: the Metropolis algorithm. *Journal of Hydrology* **211**: 69–85.

Kuntiyawichai K, Schultz B, Uhlenbrook S, Suryadi FX, Van Griensven A. 2011. Comparison of flood management options for the Yang River Basin, Thailand. *Irrigation and Drainage* **60**: 526–543.

Larose M, Heathman GC, Norton LD, Engel B. 2007. Hydrologic and atrazine simulation of the Cedar Creek Watershed using the SWAT model. *Journal of Environmental Quality* **36**: 521–531.

Lin Z, Radcliffe DE. 2006. Automatic calibration and predictive uncertainty analysis of a semidistributed watershed model. *Vadose Zone Journal* **5**: 248–260.

Metropolis N, Rosenbluth AW, Rosenbluth MN, Teller AH, Teller E. 1953. Equation of state calculations by fast computing machines. *The Journal of Chemical Physics* **21**: 1087–1092.

Moriasi DN, Arnold JG, Van Liew MW, Bingner RL, Harmel RD, Veith TL. 2007. Model evaluation guidelines for systematic quantification of accuracy in watershed simulations. *Transactions of the Asabe* **50**: 885–900.

Nash J., Sutcliffe JV. 1970. River flow forecasting through conceptual models part I—A discussion of principles. *Journal of hydrology* **10**(3), 282–290.

Ndomba P, Mtalo F, Killingtveit A. 2008. SWAT model application in a data scarce tropical complex catchment in Tanzania. *Physics and Chemistry of the Earth* **33**: 626–632.

Neitsch SL, Arnold JG, Kiniry JR, Williams JR. 2011. Soil and water assessment tool, theoretical documentation, version 2009. Texas Water Resources Institute Technical Report No. **406**.

Phomcha P, Wirojanagud P, Vangpaisal T, Thaveevouthti T. 2011. Predicting sediment discharge in an agricultural watershed: a case study of the Lam Sonthi watershed, Thailand. *ScienceAsia* **37**: 43–50.

Reungsang P, Kanwar RS, Srisuk K. 2010. Application of SWAT model in simulating stream flow for the Chi River Subbasin II in northeast Thailand. *Trends Research in Science and Technology* **2**: 23–28.

Rossi CG, Srinivasan R, Jirayoot K, Le Duc T, Souvannabouth P, Binh N, Gassman PW. 2009. Hydrologic evaluation of the lower Mekong river basin with the soil and water assessment tool model. *International Agricultural Engineering Journal* **18**: 1–13.

Sangchan W, Bannwarth MA, Ingwersen J, Hugenschmidt C, Schwadorf K, Thavornyutikarn P, Pansombat K, Streck T. Monitoring and risk assessment of pesticides in a tropical river of an agricultural watershed in northern Thailand, submitted to Environmental Monitoring and assessment.

Sangchan W, Hugenschmidt C, Ingwersen J, Schwadorf K, Thavornyutikarn P, Pansombat K, Streck T. 2012. Short-term dynamics of pesticide concentrations and loads in a river of an agricultural watershed in the outer tropics. *Agriculture, Ecosystems and Environment* **158**: 1–14.

Schreinemachers P, Sirijinda A. 2008. Pesticide use data for the Mae Sa watershed, Thailand. Report within the SFB 564: Sustainable Land Use and Rural Development in Mountainous Regions of Southeast Asia, University of Hohenheim, Germany.

Schreinemachers P, Sringarm S, Sirijinda A. 2011. The role of synthetic pesticides in the intensification of highland agriculture in Thailand. *Crop Protection* **30**: 1430–1437.

Schuler U. 2008. Towards regionalisation of soils in northern Thailand and consequences for mapping approaches and upscaling procedures. Hohenheimer Bodenkundliche Hefte89,.

Schuol J, Abbaspour KC, Yang H, Srinivasan R, Zehnder AJB. 2008. Modeling blue and green water availability in Africa. *Water Resources Research* **44**(7), doi: 10.1029/2007WR006609.

Setegn SG, Srinivasan R, Melesse AM, Dargahi B. 2010. SWAT model application and prediction uncertainty analysis in the Lake Tana Basin, Ethiopia. *Hydrological Processes* **24**: 357–367.

Shen ZY, Chen L, Chen T. 2012. Analysis of parameter uncertainty in hydrological and sediment modeling using GLUE method: a case study of SWAT model applied to Three Gorges Reservoir Region, China. *Hydrology and Earth System Sciences* **16**: 121–132.

Strauch M, Bernhofer C, Koide S, Volk M, Lorz C, Makeschin F. 2012. Using precipitation data ensemble for uncertainty analysis in SWAT streamflow simulation. *Journal of Hydrology* **414-415**: 413–424.

Tripathi MP, Panda RK, Raghuwanshi NS. 2003. Identification and prioritisation of critical sub-watersheds for soil conservation management using the SWAT model. *Biosystems Engineering* **85**: 365–379.

Ullrich A, Volk M. 2010. Influence of different nitrate-N monitoring strategies on load estimation as a base for model calibration and evaluation. *Environmental Monitoring and Assessment* **171**: 513–527.

van Griensven A, Meixner T. 2007. A global and efficient multi-objective auto-calibration and uncertainty estimation method for water quality catchment models. *Journal of Hydroinformatics* **9**: 277–291.

van Griensven A, Meixner T, Grunwald S, Bishop T, Diluzio A, Srinivasan R. 2006. A global sensitivity analysis tool for the parameters of multi-variable catchment models. *Journal of Hydrology* **324**: 10–23.

Wickel AJ, van de Giesen NC, Sá TDA. 2008. Stormflow generation in two headwater catchments in eastern Amazonia, Brazil. *Hydrological Processes* **22**: 3285–3293.

Yang J, Reichert P, Abbaspour KC, Xia J, Yang H. 2008. Comparing uncertainty analysis techniques for a SWAT application to the Chaohe Basin in China. *Journal of Hydrology* **358**: 1–23.

Ziegler AD, Benner S, Tantasarin C, Jachowski NR, Wood SH, Sutherland RA, Lu XX, Giambelluca TW, Nullet MA. Sediment load estimation using automated turbidity-based sediment monitoring in the Mae Sa catchment in northern Thailand submitted to River Research and Applications.

Ziegler AD, Bruun TB, Guardiola-Claramonte M, Giambelluca TW, Lawrence D, Thanh Lam N. 2009. Environmental consequences of the demise in swidden cultivation in Montane Mainland Southeast Asia: hydrology and geomorphology. *Human Ecology* **37**: 361–373.

Ziegler AD, Negishi JN, Sidle RC, Gomi T, Noguchi S, Nik AR. 2007. Persistence of road runoff generation in a logged catchment in Peninsular Malaysia. *Earth Surface Processes and Landforms* **32**: 1947–1970.

